

6th International Conference on Silicon Photovoltaics, SiliconPV 2016

Carrier lifetime in liquid-phase crystallized silicon on glass

Michael Vetter*, Annett Gawlik, Jonathan Plentz, Gudrun Andrä

Leibniz-Institute for Photonic Technology (IPHT), Department Functional Interfaces, Albert-Einstein-Str. 9, D-07745 Jena, Germany

Abstract

Liquid-phase crystallized silicon on glass (LPCSG) presents a promising material to fabricate high quality silicon thin films, e.g. for solar cells and modules. Barrier layers and a doped amorphous silicon layer are deposited on the glass substrate followed by crystallization with a line focus laser beam. In this paper we introduce injection level dependent lifetime measurements generated by the quasi steady-state photoconductance decay method (QSSPC) to characterize LPCSG absorbers. This contactless method allows a determination of the LPCSG absorber quality already at an early stage of solar cell fabrication, and provides a monitoring of the absorber quality during the solar cell fabrication steps. We found minority carrier lifetimes higher than 200 ns in our layers (e.g. n-type absorber with $N_D=2 \times 10^{15} \text{ cm}^{-3}$) indicating a surface recombination velocity $S_{BL} < 3000 \text{ cm/s}$ at the barrier layer/Si interface.

© 2016 The Authors. Published by Elsevier Ltd. This is an open access article under the CC BY-NC-ND license (<http://creativecommons.org/licenses/by-nc-nd/4.0/>).

Peer review by the scientific conference committee of SiliconPV 2016 under responsibility of PSE AG.

Keywords: multicrystalline silicon; thin film; laser crystallization; carrier lifetime; quasi steady-state photoconductance

1. Introduction

Laboratory solar cells implementing liquid-phase crystallized silicon on glass (LPCSG) produced by line focus laser beam or electron beam (e-beam) crystallization of amorphous silicon (a-Si) layers on glass, showed open circuit voltages (V_{oc}) over 600 mV [1-5] making closer the gap of thin film crystalline silicon solar cells to multi-crystalline silicon wafer solar cells [6]. LPCSG presents a promising material to fabricate solar cells and modules, this technology could merge the advantages of crystalline silicon (c-Si) wafer technology with its high efficiency potential and thin film technology with low Si consumption and low cost monolithic integration for module

* Corresponding author. Tel.: +49 (0)3641 206 438; fax: +49 (0)3641 206 499.
E-mail address: michael.vetter@leibniz-ipht.de

fabrication. LPCSG technology could be an approach to overcome the emerging limits for further cost reduction in standard wafer-based module technology as e.g. reduction of wafer thickness or increasing wafer size.

The introduction of barrier layers (BL) between the glass and the Si layer plays an important role in achieving a high electronic material quality after the crystallization process. The BLs must ensure good adhesion of Si (wettability), facilitating crystallization of high-quality Si, blocking diffusion of impurities from the glass, passivating Si interface defects and acting as a transparent antireflection coating for the superstrate configuration, furthermore it could serve as a dopant source for the absorber. Recent investigations were focused on combination of SiO₂, SiN_x, SiO_xN_y and SiC_x layers [7, 8] however, a combination fulfilling all the requirements is still objective of investigation.

Most developments of the LPCSG absorbers have been made by fabricating solar cells, measuring and analyzing current-voltage (IV) characteristics and quantum efficiency (QE) or on quasi-solar cells measuring the Suns-V_{oc} characteristic. In this paper, we introduce the measurement and analysis of injection level dependent lifetime (τ) measurements generated by the quasi steady-state photoconductance decay (QSSPC) method [9]. This contactless method provides information on the LPCSG absorber quality already at an early stage of solar cell fabrication, and a way to monitor the absorber quality during the solar cell fabrication steps.

In literature [1] the effective diffusion length (L_{eff}) of high-quality LPCSG absorbers is estimated from QE data to lie around 10-30 μm for solar cells with absorber thickness (W) in the range of $W=5-10 \mu\text{m}$ and with efficiency in the range of 10%. Carrier lifetime can be calculated from the basic relation $\tau_{eff} = L_{eff}^2/D$ and diffusion constant $D = \mu_{eff}kT/q$ where μ_{eff} is the effective carrier mobility. In Figure 1 this relation is shown for c-Si where μ , D and τ are calculated by using the “mobility calculator” on the pvlighthouse web page [10]. The relation of L_{eff} and τ_{eff} is shown for different n-type doping densities (N_D) and at an injection level (Δn) of 10^{15} cm^{-3} . In addition, the relation is calculated for $N_D=2 \times 10^{16} \text{ cm}^{-3}$ for $\Delta n=10^{13} \text{ cm}^{-3}$, presenting no dependence on injection level for c-Si (in this range). Since the dependence of μ on doping concentration in LPCSG seems to be somewhat different to c-Si [1] the relation will be slightly different, nevertheless Figure 1 suggests that for $L_{eff} \approx 10-30 \mu\text{m}$ [1] τ_{eff} of n-type LPCSG absorbers ($W \approx 5-10 \mu\text{m}$) is in the range from a few ns to 1 μs .

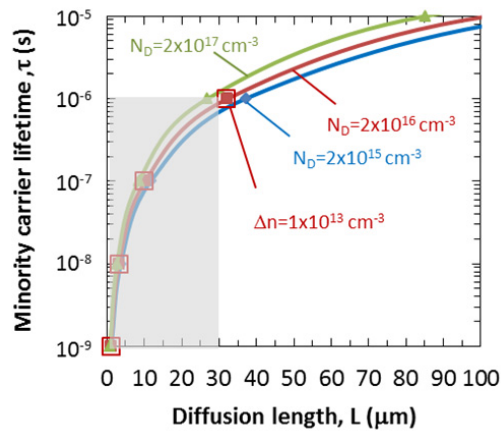


Fig. 1. From the lifetime-(ambipolar) diffusion length relation of c-Si (injection level $\Delta n=1 \times 10^{15} \text{ cm}^{-3}$, red open squares: $\Delta n=1 \times 10^{13} \text{ cm}^{-3}$ for $N_D=2 \times 10^{16} \text{ cm}^{-3}$), considering the lower mobility in LPCSG and the estimation of the $L_{eff} \approx 10-30 \mu\text{m}$ [1] we estimate lifetimes for LPCSG absorbers to be in the range of a few ns to 1 μs (marked area in the figure).

2. Experimental

LPCSG absorbers are prepared on Borofloat 33 (Schott) glasses (see Figure 2 left, upper part). At first BLs are deposited by sputtering or chemical vapor deposition. Then, n-doped a-Si layers (5-12 μm) are deposited by electron beam evaporation. The crystallization is performed by scanning with continuous wave line focus laser irradiation at 808 nm over the sample [3]. The typical preparation steps of the solar cell fabrication process are a then, surface etch and RCA cleaning after crystallization (in the following step 1), hydrogen plasma treatment (step 2), followed by a second surface etch and RCA cleaning to remove surface damage (step 3), followed by intrinsic a-Si:H deposition (step 4) and p-type a-Si:H deposition (step 5) for hetero emitter formation [11].

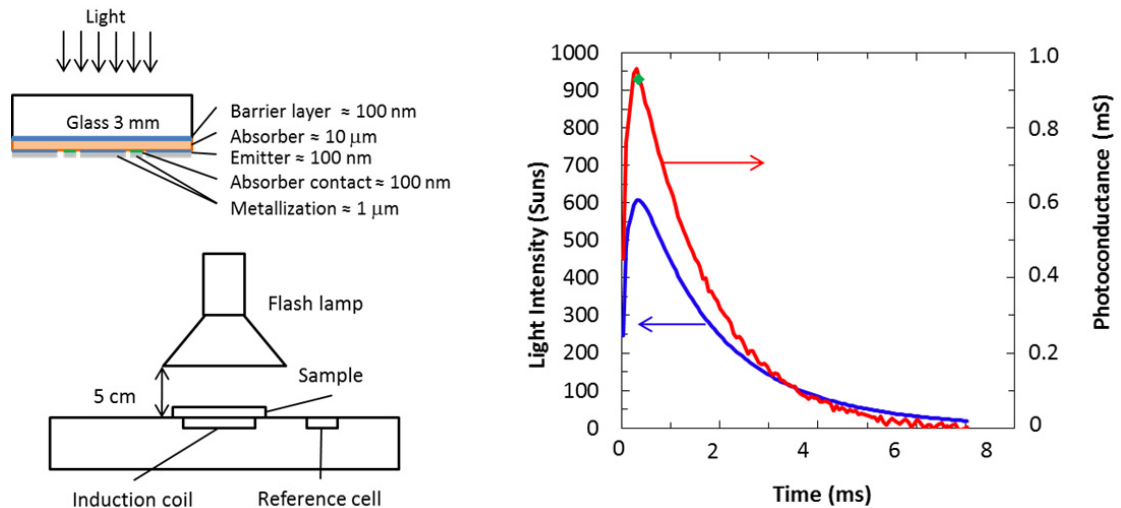


Fig. 2. Left, upper part: Solar cell structure with LPCSG absorber with layer thickness indicated. Lower part: Experimental set-up for lifetime measurement for LPCSG absorbers. Asymmetrical location of the flash prevents the saturation of the reference cell. Small distance provides high injection levels in the sample resulting in sufficient conductivity change of the thin Si layers. Right: Measurement data to calculate lifetime of sample after i-layer deposition.

To measure τ as function of the injection level (Δn) in the thin LPCSG absorbers, we modified the standard set-up of a Sinton WCT-120 Photoconductance tool (Figure 2, left). This is necessary since on the one hand, the LPCSG absorbers are very thin and therefore present much lower conductivity than standard solar cell wafers (150-300 μm thick). This results in working point of LPCSG absorbers near the detection limit of the inductive measurement bridge of the conductance tool. On the other hand τ is expected to be short and absorption low due to the small thickness which will result in rather low excess carrier densities under illumination. To overcome these difficulties we have lowered the flash lamp to sample distance to 5 cm. This position results in much higher generation rate and excess carrier density in the sample compared to the standard distance of 50 cm and sufficient change of conductivity in the sample which can be detected by the measurement bridge (Figure 2, right). In this arrangement the reference solar cell located beside the sample under investigation gets saturated in wide range of illumination. To overcome this problem we chose a lamp position with an asymmetrical illumination of sample and reference cell which has to be adjusted by a recalibration. To determine the calibration factor of this asymmetrical set-up we use the data of a well-passivated Si wafer. In addition, the optical factor to account for the different absorption properties of wafer and LPCSG substrate has to be determined, but this is out of the scope of this work and will be treated in more detail elsewhere. The calibration method introduces some error in the lifetime and open circuit voltage (V_{oc}) calculation, also the exact dependence of mobility on doping density and injection level is not well known for LPCSG material. However, the measurements allow the comparison of lifetime data of different process steps of the same sample or of samples with same or similar optical properties.

3. Results and discussion

An important prerequisite to be able to measure the lifetime in thin Si layers in the thickness range of a few μm is a very good electronic surface passivation. For insufficient passivated surfaces the surface recombination velocity (S) reaches the thermal electron/hole velocity ($v_{\text{th}}=2 \times 10^7$ cm/s). Then in the case of steady-state generation throughout the wafer thickness, the upper limit of τ_{eff} is given by $1/\tau_{\text{eff}}=1/\tau_{\text{bulk}} + 12 \cdot D/W^2$ [12], where τ_{bulk} is the lifetime of the Si absorber bulk material. From this equation, one calculates an upper limit of τ_{eff} in the range of a few ns ($N_D \approx 10^{15}-10^{17} \text{ cm}^{-3}$), and bulk lifetime will not be visible. Therefore, first we must find a barrier layer which provides sufficient good passivation at the glass Si interface, next the top surface of the absorber must be well passivated. For that purpose, after the laser-crystallization surface etching and cleaning is performed and we apply an HF-dip to the surface just before the τ measurement, which provides good surface passivation for a short time. Figure 3 shows lifetime measurements of an n-type LPCSG layer with a doping density in the range of $N_D \approx 4 \times 10^{16} \text{ cm}^{-3}$. The absorber is deposited on a BL stack consisting in a silicon nitride layer capped with a silicon oxide layer and the figure shows τ_{eff} after typical preparation steps of the solar cell fabrication process. After laser-crystallization, the Si oxide created on the top surface during the laser process is removed, and the surface is cleaned. Subsequently, τ is measured after an HF-dip and usually presents a lifetime curve similar to the one shown in Figure 3 (step1, purple dots). We observe a strong increase of τ in the range $\Delta n=10^{14}-10^{15} \text{ cm}^{-3}$, presenting high lifetimes at low injection levels (Δn). This is also known for other mc-Si materials and attributed to carriers in space charge regions at grain boundaries (depletion region modulation effect) [13] and trapping of carriers in defect states [14]. At this stage we perform an H-passivation step to reduce electronic defects applying a hydrogen plasma treatment to the samples. Subsequent measurement of τ (after having dipped the sample in HF) presents a rather short lifetime of maximum 5 ns (see Figure 3, brown squares). However, after applying a surface etch and RCA cleaning with final HF-dip, we observe that τ increases significantly up to 30 ns (Figure 3, blue rhombus). The reason for this large increase is a defect-rich surface caused by sputtering of Argon ions during the H passivation, since we have no remote plasma source available. The first step of hetero emitter preparation is the deposition of a thin intrinsic amorphous Si layer (i-Si). The lifetime curve after i-layer deposition (red triangles) only slightly changes in comparison to the passivation with hydrogen (HF-dip) indicating a similar surface passivation mechanism at the top surface. Next, we deposit a p-type amorphous Si layer (p-Si, green crosses) and observe again that the lifetime curve changes slightly indicating that the last fabrication steps also had a small impact on the recombination in the solar cell absorber. Subsequent preparation steps of the hetero emitter, e.g. the deposition of a transparent conductive oxide (TCO), are still under investigation and will be reported elsewhere.

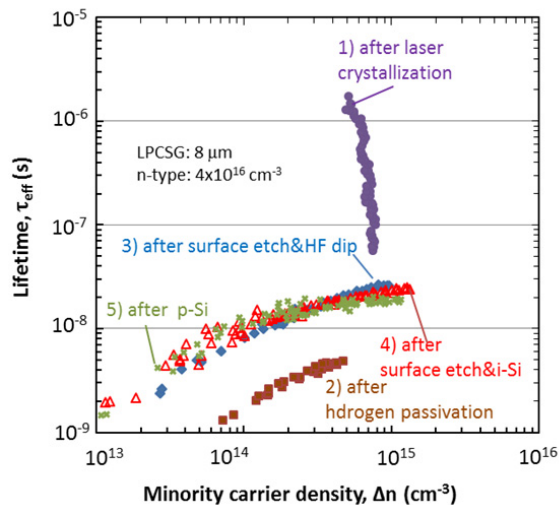


Fig. 3. Lifetime measurements of a 9 μm LPCSG absorber after different preparation steps.

Additional information about the recombination in the structure can be obtained from suns- V_{oc} curves calculated from the conductance data [15]. Figure 4 compares the calculated Suns- V_{oc} data of the fabrication steps presented in Figure 3. For each curve a logarithmic fit of the data in the high injection region is made and the respective parameters are presented in Table 1. After hydrogen passivation (step 2) the implied open circuit voltage at 1 sun is 388 mV and increases to 531 mV after p-Si layer deposition (step 5). The slope of the Suns- V_{oc} curve predicts the slope of the logarithmic solar cell current voltage curve without resistance losses. Directly after the H-passivation step the slope is nearly 120 mV/decade which indicates a diode ideality factor of nearly 2. The slope decreases to about 79 mV/decade with an $V_{oc}(1\text{sun}) = 520$ mV after the surface etch and surface cleaning of the top surface showing that the H-plasma treatment had damaged the top surface then dominating the recombination in the structure. From the data of Table 1, surface recombination is after i-layer deposition slightly higher resulting in lower $V_{oc} = 503$ mV compared to the passivation by hydrogen atoms of the HF-dip. This might be due to the still not fully optimized deposition conditions of the i-layer. i-layer also must be kept as thin as possible to obtain a high fill factor in the final solar cell therefore results still a high defect density at the surface. In the next fabrication step the p-Si layer deposition creates an electric field at the top surface increasing the implied $V_{oc}(1\text{sun})$ to 531 mV and reducing the slope of the Suns- V_{oc} curve to 69 mV/decade meaning further reduction of recombination at the top surface. The value of 69 mV/decade after p-Si layer deposition indicates already small recombination losses at high injection levels in the bulk of the absorber and at the absorber barrier layer interface.

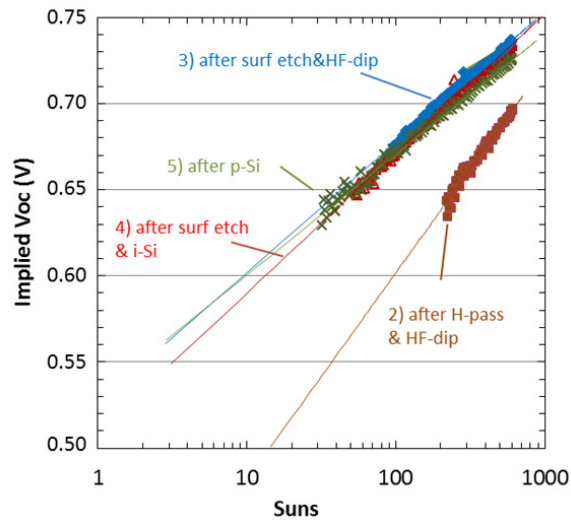


Fig. 4. Calculated Suns- V_{oc} data of the sample from Figure 3. Lines are presenting the fitting of data, fitting results are summarized in Table 1.

Table 1. Data compilation of fitting Suns- V_{oc} curves in figure 4.

Fabrication step	$V_{oc}(1\text{sun})$ (mV)	Slope (suns- V_{oc}) (mV/decade)
after H-Passivation&HF-dip	388	111
after surface etch&HF-dip	520	79
after i -layer deposition	503	83
after p -layer deposition	531	69

Figure 5 presents the lifetime data of two n-type LPCSG absorbers with a very small thickness of only 5 and 6 μm and with doping density of approx. $2 \times 10^{16} \text{ cm}^{-3}$ and $2 \times 10^{15} \text{ cm}^{-3}$ respectively, which still provide sufficient conductivity for measurement with the WCT-120 tool at high injection levels. Surface passivation of both samples is performed by HF-dip after surface etching and RCA cleaning. The lower doped sample (Figure 5, blue squares) presents an approximately ten times higher lifetime (up to 200 ns) than the higher doped sample suggesting a similar relationship between lifetime and doping density as known for c-Si wafers. The higher lifetime of this sample coincides with higher maximum injection levels and shifts the injection level of 1 sun (indicated by the arrow and implied V_{oc}) into the measurable range of the conductance tool. However, the sensitivity of the conductance tool is limiting data acquisition at low injection levels and the available data range is small, making simulation and data fitting difficult. Further information of the underlying recombination mechanism in the absorber structure from data simulation would help to understand how to improve the absorber quality. Nevertheless, the high surface passivation quality of HF-dip samples shown in figure 3 suggests that the remaining recombination in the absorber structure is due to bulk recombination and recombination at the barrier layer interface. If we assume that the surface recombination at the top surface is very small (as e.g. determined on n-type wafers), then on the one hand, an upper limit of the effective surface recombination velocity (S_{BL}) at the BL-Si interface can be estimated by $1/\tau_{eff} = 1/\tau_{bulk} + S_{BL}/W$. For the LPCSG absorber in Figure 5 (blue squares), the τ_{eff} of about 200 ns then indicates an upper limit of the S_{BL} of about 3000 cm/s when τ_{bulk} increases to infinity. On the other hand, attributing all recombination to the BL interface Figure 1 indicates a diffusion length in the range of 10 μm for this structure.

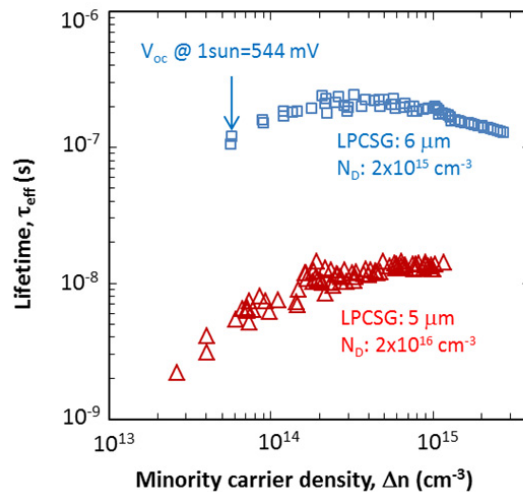


Fig. 5. Lifetime data of two LPCSG absorbers with different n-type doping with only 5 and 6 μm thickness. The higher lifetime of the lower doped sample (blue squares) results in higher maximum injection level and also shifts the injection level of 1 sun marked by an arrow in the detectable range of the conductance tool.

4. Conclusion

We have shown that by small modifications of the WCT-120 photoconductance tool and respective recalibrations for data analysis it is possible to generate lifetime data and calculate Suns- V_{oc} curves at high injection levels for very thin silicon absorber layers. However, the data includes still uncertainties due to variations in the optical absorption (i.e. the optical factor included in the calculations) of the thin absorbers and to the lack of carrier mobility data of LPCSG material. The determination of mobility data in function of doping concentration and injection level of LPCSG material is focus of ongoing research. Nevertheless, lifetime of LPCSG absorber at high injection levels was found to be in the range estimated from reported diffusion lengths. The data provides already information about surface and bulk quality of the thin absorbers and the impact of process steps in solar cell fabrication.

Acknowledgements

The authors like thank H.-P. Linke and U. Brückner for technical assistance. This project has received funding from the European Union's Horizon 2020 research and innovation programme under the Marie Skłodowska-Curie grant agreement No 657115 (cSiOnGlass, M.V.).

References

- [1] J. Haschke, D. Amkreutz, L. Korte, F. Ruske, B. Rech B, "Towards wafer quality c-Si thin-film solar cells on glass", *Sol. Energy Mater. Solar Cells* 128, 190-197 (2014).
- [2] J. Dore, D. Ong, S. Varlamov, R. Egan, M.A.Green, "Progress in laser-crystallized thin-film polycrystalline silicon solar cells: intermediate layers, light trapping, and metallization, *IEEE J. Photovolt.* 4 (1) 33-39 (2014).
- [3] A. Gawlik, I. Höger, J. Bergmann, J. Plentz, T. Schmidt, F. Falk, G. Andrä, "Optimized emitter contacting on multicrystalline silicon thin film solar cells", *Phys. Status Solidi RRL* 9 (7), 397-400 (2015).
- [4] G. Jia, G. Andrä, A. Gawlik, S. Schönherr, J. Plentz, B. Eisenhawer, T. Pliewischkies, A. Dellith, F. Falk, Nanotechnology enhanced solar cells prepared on laser-crystallized polycrystalline thin films (<10 µm), *Sol. Energy Mater and Solar Cells* 126 (2014) 62-67.
- [5] M. Junghanns, J. Plentz, G. Andrä, A. Gawlik, I. Höger, F. Falk, PEDOT:PSS emitters on multicrystalline silicon thin-film absorbers for hybrid solar cells, *Appl. Phys. Lett.* 106 (2015) 083904-1-3.
- [6] M. A. Green, K. Emery, Y. Hishikawa, W. Warta, E. D. Dunlop, "Solar cell efficiency tables (version 46)", *Progr. Photovol. Res. Appl.* 23, 805-812 (2015).
- [7] O. Gabriel, T. Frijnts, S. Calnan, S. Ring, S. Kirner, A. Opitz, I. Rothert, H. Rhein, M. Zelt, K. Bhatti, J-H Zollondz, A. Heidelberg, J Haschke, D. Amkreutz, S. Gall, F. Friedrich, B. Stannowski, B. Rech, R. Schlatmann, "PECVD Intermediate and absorber layers applied in liquid-phase crystallized Si solar cells on glass substrates", *IEEE J. Photovolt.* 4 (6) 1343-1348 (2014).
- [8] J. Dore, S. Varlamov, M.A. Green, "Intermediate layer development for laser-crystallized thin-film Si solar cells on glass", *IEEE J Photovolt.* 5 (1), 9-16 (2015).
- [9] R. Sinton, A. Cuevas "Contact-less determination of current-voltage characteristics and minority carrier lifetimes in semiconductors from quasi steady-state photoconductance data", *Appl. Phys. Lett.* 69, 2510 (1996).
- [10] <https://www.pvlighthouse.com.au/calculators/mobility%20calculator/mobility%20calculator.aspx>.
- [11] I. Höger, M. Himmerlich, A. Gawlik, U. Brückner, S. Krischok, G. Andrä, *J. Appl. Phys.* 119, 045306 (2016), Influence of intermediate layers on the surface condition of laser crystallized silicon thin films on solar cell performance.
- [12] I. Martin, Thesis (2003, Universitat Politècnica de Catalunya, Barcelona, Spain) p. 45.
- [13] C. Leendertz, A.-M. Teodoreanu, L. Korte, and B. Rech, *J. Appl. Phys.* 113 (2013) 044510, The influence of space charge regions on effective charge carrier lifetime in thin films and resulting opportunities for materials characterization.
- [14] A. Cuevas, M. Stocks, D McDonald; M. Kerr; C. Samundsett, *IEEE Trans. Electr.* 46 (1999) 2026, Recombination and trapping in multicrystalline silicon.
- [15] R.A. Sinton, A. Cuevas, *Appl. Phys. Lett.* 69 (1996) 457, Contactless determination of current-voltage characteristics and minority carrier lifetime in semiconductors from quasi-steady-state photoconductance data.